The laminar boundary layer on a rotating wind turbine blade

Horia DUMITRESCU[*], Vladimir CARDOŞ[*], Alexandru DUMITRACHE[*] and Florin FRUNZULICĂ[**]

*"Gh. Mihoc, C. Iacob" Institute of Statistical Mathematics and Applied Mathematics of the Romanian Academy, Bucharest, Calea 13 Septembrie No. 13, Bucharest 050711, Romania
v_cardos@yahoo.ca
**Department of Aerospace Sciences, POLITEHNICA University Bucharest
Splaiul Independenței 313, 060042, Bucharest, Romania
DOI: 10.13111/2066-8201.2010.2.2.6

Abstract: *The present paper describes a method to calculate velocity profiles in the boundary layer of rotating blade. A differential approach is used to solve the laminar boundary layer equations. The effects of tip speed ratio, dimensionless radial position r/R and angle of attack have been analyzed. The test airfoils used in the simulations are NACA 63-215 and S809. The resulting velocity profiles in the chordwise and spanwise directions are mapped and stored in a Database according to the boundary layer parameters.*

Key Words: Vortex dynamics; Wind turbine; Numerical simulation.

1. INTRODUCTION

Accurate prediction of the wind turbine performance is mandatory for designing new wind turbine blades. This demands access to accurate and fast CFD tools, such advanced Navier-Stokes solvers or viscous-inviscid interactive codes. Most of the existing CFD codes assume that the boundary layer is completely turbulent or employ inadequate or oversimplified criteria for the prediction of laminar-turbulent transition. The laminar-turbulent transition process is related to the stability of the boundary layer, and rotational effects must be included in the stability analysis of the velocity profiles. It is the aim of the present work to establish a Database of velocity profiles on rotating wings that can be used in subsequent analysis as base flow either to a stability analysis or to an integral boundary layer formulation.

Three dimensional boundary layer equations have been extensively studied; a very complete review by Hansen [1] explains in detail the principle of the similarity analysis for the boundary layer equations. Cooke [2] gives a summary of the first approximation to 3-dimensional boundary layers.

The inconvenience of the previous work is that rotational effects are not included. The formulation of the boundary layer equations in a rotating reference frame was given by Snel [3] in order to carry out an order of magnitude analysis and to develop a quasi-3-dimensional formulation that includes rotational effects.

[*] Tel: +40213182433; fax: +40213182439.
E-mail address: v_cardos@yahoo.ca; *URL:* http://www.ima.ro

In the present work the boundary layer parameters are calculated from the integral formulation by Mager [4]. Two different approaches can be used to calculate the velocity profiles: the momentum integral and the differential approach. If an integral approach is used a reasonable assumption of the velocity profiles needs to be defined. In contrast, if a differential approach is used the exact velocity profile is found as a part of the solution. This is the idea behind the Blasius solution on a flat plate and its generalization for positive and adverse pressure gradients using the Falkner-Skan solution. A similarity variable transformation technique applied to the boundary layer equations that includes three dimensional and rotational effects, i.e. the Coriolis and centrifugal forces, have been studied by [5] and [6]. The main advantage of using the similarity variable transformation technique is that the equations only need to be solved once, because they cover the full range of Reynolds numbers. A database approach is used to map the velocity profiles that in a future work will be used for the stability analysis to calculate the transition from laminar to turbulent flow.

2. NUMERICAL METHOD

For a rotating wind turbine blade (see Figure 1), the three-dimensional boundary layer equations can be obtained from the incompressible Navier-Stokes equations in curvilinear coordinates using boundary layer approximations. To solve the differential boundary layer equations, the common way is to find a similarity variable to regroup the equations and then integrate the final equations using some numerical techniques. Unfortunately, it is very difficult or even impossible to find a common similarity variable for the three-dimensional boundary layer equations of a rotating blade. In 2003, Dumitrescu and Cardos [5] presented a similarity approach to solve the three-dimensional boundary layer of a rotating wing consisting of flat plates whose leading edges are set in the radial direction.

Considering a sectional cut, the similarity formulation was achieved for a flat plate aligned with the azimuth direction in the cylindrical coordinates. Since a flat plate wing is not used for wind turbines, it is thus needed to extend a technique to solve the three-dimensional boundary layer of a wind turbine wing by using a similar tool developed in [5]. In the following, the quasi-3D boundary layer equations together with a similarity approach for a general flat plate are described in 2.1 and the quasi-3D approach for an airfoil using the theory for a flat plate is discussed in 2.2. Initial conditions are discussed in 2.3 and followed by numerical integrations in 2.4.

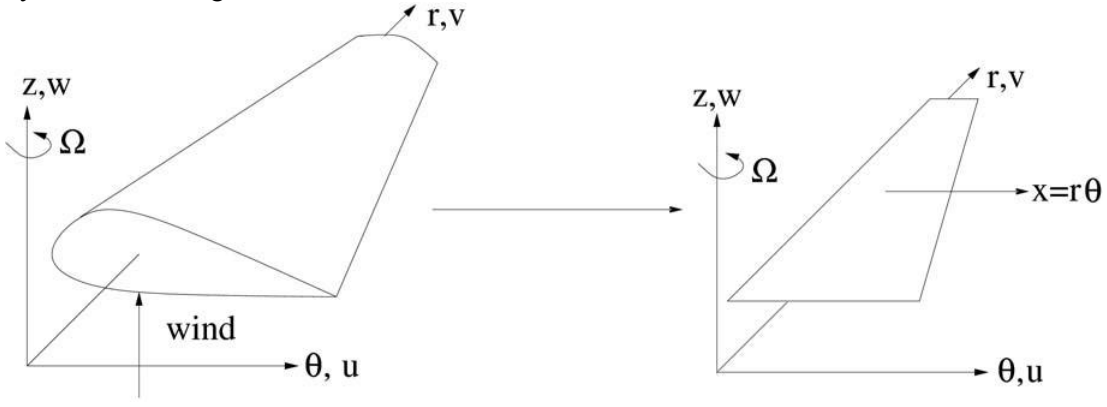

Fig. 1 – Reference system for a rotating wing.

2.1. Boundary layer equations for a flat wing

In this section, the boundary layer equations for a rotating flat wing are presented. For a rotating wind turbine wing, it is preferable to use cylindrical coordinates where the origin is chosen at the rotor center and the radial axis passes the positions of 1/4 chords from the leading edge (see Figure 1). In the system, the wing is rotating with an angular velocity of Ω around the *z*-axis and the wind comes from the negative direction of *z*. In order to achieve a similarity variable, the real wing is transformed to a flat wing aligned with the azimuth direction (see also Figure 1). In the cylindrical coordinates the steady laminar incompressible boundary layer equations are expressed

$$\frac{1}{r}\frac{\partial u}{\partial \theta}+\frac{v}{r}+\frac{\partial v}{\partial r}+\frac{\partial w}{\partial z}=0\,, \tag{1}$$

$$\frac{u}{r}\frac{\partial u}{\partial \theta}+v\frac{\partial u}{\partial r}+w\frac{\partial u}{\partial z}=-\frac{1}{\rho r}\frac{\partial p}{\partial \theta}+\frac{1}{\rho}\frac{\partial \tau_\theta}{\partial z}+2\Omega v-\frac{uv}{r}\,, \tag{2}$$

$$\frac{u}{r}\frac{\partial v}{\partial \theta}+v\frac{\partial v}{\partial r}+w\frac{\partial v}{\partial z}=-\frac{1}{\rho}\frac{\partial p}{\partial r}+\frac{1}{\rho}\frac{\partial \tau_r}{\partial z}+\frac{\left(u-\Omega r\right)^2}{r}\,, \tag{3}$$

where *u*, *v*, and *w* are the velocity components in the θ, *r* and *z* directions, respectively, *p* is the pressure, and τ_r and τ_θ are the wall shear stresses in the radial and tangential directions, respectively. The pressure gradient is found from the equations by applying the equations at the edge of a boundary layer with $u=U$ and $v=0$.

Before introducing similarity variables, two cases are needed to be considered. The first case (Case1) comprises the area from the stagnation point to the leading edge and the second one (Case 2) counts from the leading edge to the trailing edge on the suction side. In order to use the method presented in [5], the following transformations are used

$$\text{Case 1: } x=x_s-r\theta,\ \xi=\frac{x}{c}=\frac{x_s-r\theta}{c},\ \eta=-z\sqrt{\frac{U}{xv}}\,,$$

$$\text{Case 2: } x=r\theta+x_s-2x_l,\ \xi=\frac{x}{c}=\frac{r\theta+x_s-2x_l}{c},\ \eta=z\sqrt{\frac{U}{xv}}\,,$$

where x_s and x_l are the θ-coordinate of the stagnation point and the leading edge, respectively, and *U* is the edge velocity at the edge of a boundary layer that is a function of *r* and θ. Using the similarity variables, the velocity is expressed as

$$\text{Case 1: } u=-Uf'\left(\xi,\eta\right)=-U\frac{\partial f}{\partial \eta},\ v=Ug'\left(\xi,\eta\right)=U\frac{\partial g}{\partial \eta},$$

$$\text{Case 2: } u=Uf'\left(\xi,\eta\right)=U\frac{\partial f}{\partial \eta},\ v=Ug'\left(\xi,\eta\right)=U\frac{\partial g}{\partial \eta}.$$

Substituting the velocity definitions using the similarity variables to the boundary layer equations, the following PDE system is obtained

$$f'''+0.5ff''+\xi f_\xi f''+\frac{c}{r}\xi gf''-\xi f_\xi' f'+m\left(1+0.5ff''-f'^2\right)+n\left(0.5f''g-f'g'\right)+$$
$$+2s_w\frac{c}{r}\xi g'\left(\frac{\Omega r}{U}\right)-\frac{c}{r}\xi g'f'+s_w f''\frac{\theta}{2}g+s_w\xi\theta f''g_\xi-s_w\xi\theta g'f'_\xi=0 \quad (4)$$

$$g'''+0.5fg''+\xi f_\xi g''+\frac{c}{r}\xi gg''-\xi g_\xi' f'+m\left(0.5fg''-f'g'\right)+n\left(0.5gg''-g'^2\right)+$$
$$+\xi\frac{c}{r}\left(1-f'^2\right)-2s_w\frac{c}{r}\xi\left(\frac{\Omega r}{U}\right)\left(f'-1\right)+s_w g''\frac{\theta}{2}g+s_w\xi\theta g''g_\xi-s_w\xi\theta g'g'_\xi=0 \quad (5)$$

where m and n are the pressure gradients in the azimuth and radial directions, respectively, s_w is the sign function that is equal to -1 in Case 1 and 1 in Case 2, and subscript with ξ designates the derivatives with respect to ξ .

Equations (4) and (5) are solved with the following boundary conditions:

$$\text{at } \eta=0,\quad f(\xi,0)=0,\ f'(\xi,0)=0,\ g(\xi,0)=0,\ g'(\xi,0)=0. \quad (6)$$

$$\text{at } \eta=\infty,\quad f'(\infty)=1,\ g'(\infty)=0. \quad (7)$$

2.2. Solving the boundary layer of a real wing

As we know that the true boundary layer equations of a rotating wind turbine wing are complicated, one way to solve the boundary layer is to use the equations (4) and (5) but with some changes. From the similarity approach made by Blasius in 1908 for the 2D boundary layer equations of a flat plate, Falkner and Skan developed in 1931 a more general similarity approach for wedge flows. Their final equation is very similar to the equation for a flat plate but with a term of pressure gradient. The idea can be generalized for a rotating blade (see Figure 2) by:

1. The equations (4) and (5) are used with true pressure gradients m and n.
2. The coordinate x needs to be used as the arc length.
3. The centrifugal and Coriolis forces should take true values at a blade.
4. The minimum point in the azimuth direction is considered as the leading edge of a flat plate in the transformation.

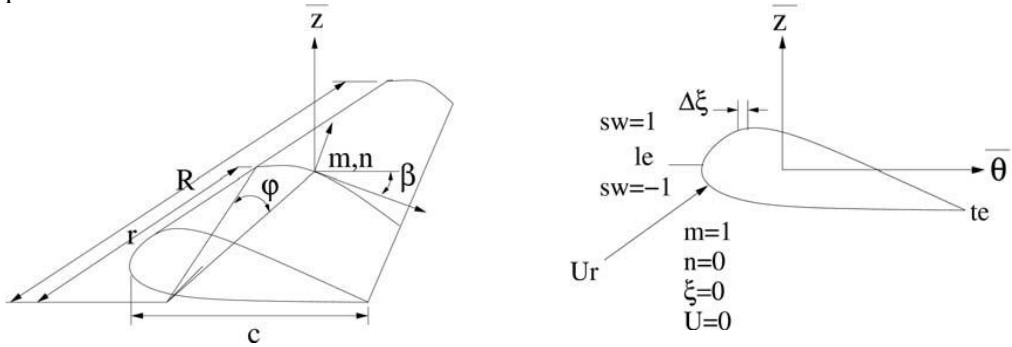

Fig. 2 – Coordinate system attached to the blade.

The dimensionless pressure-gradient parameters on the chordwise and spanwise directions at a given *r*/*R* and ξ position are found

$$m = \frac{\xi}{U_e}\frac{dU_e}{ds}\frac{1}{S_l}, \tag{8}$$

$$n = \frac{\xi c}{U_e}\frac{\partial U_e}{\partial r}, \tag{9}$$

where S_t is the total arc length from the leading edge to the trailing edge and U_e is the edge velocity. In order to find the edge velocity, the reference velocity at a point on a rotating wind turbine blade is

$$U_r = U_\infty \sqrt{\left(\lambda\frac{r}{R}\right)^2 + (1-a)^2}, \tag{10}$$

where U_∞ is the wind speed, $\lambda = \frac{\Omega R}{U_\infty}$ is the tip-speed-ratio, *R* is the radius of the turbine and *a* is the axial induced velocity interference factor. From the data of induced velocity [7] *a* is a function of the tip speed ratio λ .

From the idea of Fogarty and Sears [8], an inviscid edge velocity can be calculated as

$$U = \Omega r\varphi_{1\theta}(\theta, z) + U_\infty \varphi_{2\theta}(\theta, z), \tag{11}$$

$$V = \Omega\left[\varphi_1(\theta, z) - 2\theta\right], \tag{12}$$

$$W = \Omega r\varphi_{1z}(\theta, z) + U_\infty \varphi_{2z}(\theta, z), \tag{13}$$

where *U*, *V* and *W* represent the velocity components in the reference system defined in Figure 1. $\varphi_1(\theta, z)$ and $\varphi_2(\theta, z)$ denote the 2D potential solutions, that are constant at all radial positions. The interesting point regarding to this set of equations is that the spanwise component *V* can be derived from the local 2-dimensional velocity potential. However, this spanwise component is very small and thus neglected in the present study. The potential edge velocity components can be approached as:

$$U_e = U_r U_{xfoil}, \tag{14}$$

$$V = 0. \tag{15}$$

U_{xfoil} is the velocity obtained from the inviscid XFOIL [9] for flow past a 2D airfoil with a unit free stream velocity.

2.3. Initial Conditions

In order to solve the equations (4) and (5), an initial condition or the solution at a starting point needs to be found. For flow past an airfoil of a wind turbine blade, the starting point

would be the stagnation point. The initial velocity profile is dependent on the blade radius *R*, the local chord *c*, the tip speed ratio λ and the angle of attack α but is not dependent on the airfoil geometry. In the area near the stagnation point, the flow is symmetrical on both sides of the stagnation line and the dimensionless pressure-gradient parameter m is equal to 1 as in the case of flow against a wall (see also Figure 2).

Based on these observations, the Partial Differential Equations (4) and (5) are degenerated to a set of Ordinary Differential Equations

$$f'''+0.5ff''+\left(1+0.5ff''-f'^2\right)-2\left(c\lambda/R\right)g'=0\,, \tag{16}$$

$$g'''+0.5fg''+\left(0.5fg''-f'g'\right)+2\left(c\lambda/R\right)\left(f'-1\right)\cos\left(\beta-\gamma\right)=0\,. \tag{17}$$

If we know the position of a cross-sectional airfoil, the local angle of attack and the tip-speed ratio, a velocity profile $\left(f_p^{'},g_p^{'}\right)$ can be obtained by solving the equations (10) (11). This profile will be used as an initial guess for integrating the equations (4) and (5) with modifications.

2.4. Numerical integrations

The numerical technique used to solve the set of PDE system is a collocation method that uses the 3-stage Lobatto IIIa formula and the collocation polynomial provides continuous solution that is fourth order accurate [10]. This approach is found to be more stable that the classical shooting method that combines the Keller's box and the Newton linearization technique. The resulting PDE set is solved on the blade for different transversal cuts (r/R). Two test airfoils of constant chord: NACA 63-215 and S809 were used in the simulations. A Database was built up with 40 middle radial cuts with the angle of attack ranging between 0^0 and 20^0 and the tip-speed-ratio ranging between 3 and 12.

In order to determine the boundary layer correlations, the boundary layer parameters used by Mager are adopted. The displacement and momentum thickness in the chordwise direction are defined as

$$\delta_\theta=\int_0^\eta\left(1-f'\right)d\eta \qquad \theta_\theta=\int_0^\eta\left(1-f'^2\right)d\eta\,. \tag{18-19}$$

The cross flow parameters are calculated as

$$\delta_r=\int_0^\eta g'd\eta \qquad \theta_r=\int_0^\eta g'^2\,d\eta\,. \tag{20-21}$$

The shape factors in the chordwise and spanwise directions are defined as $H_\theta=\delta_\theta/\theta_\theta$ and $H_r=\delta_r/\theta_r$. The skin friction coefficient in the chordwise and spanwise directions are defined as follows:

$$f''(0)=\frac{1}{2}C_{f,u}\sqrt{\mathrm{Re}_x} \qquad g''(0)=\frac{1}{2}C_{f,v}\sqrt{\mathrm{Re}_x}\,. \tag{22-23}$$

3. RESULTS AND DISCUSSION

The variation of the parameter m at different angles of attack α is shown in Figures 3 and 4 for the tested airfoils. The shape factor on the chordwise and spanwise directions Hₒ and Hr are plotted in Figures 5 and 6, is seen that they are independent of the radial position (r/R) and λ However, they are dependent on the parameter m. However, small variations are observed before separation occurs.

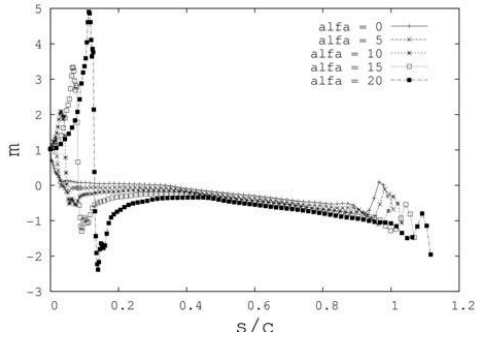

Fig, 3 – Variation of the parameter m with x/c at different angles of attack NACA 63-215

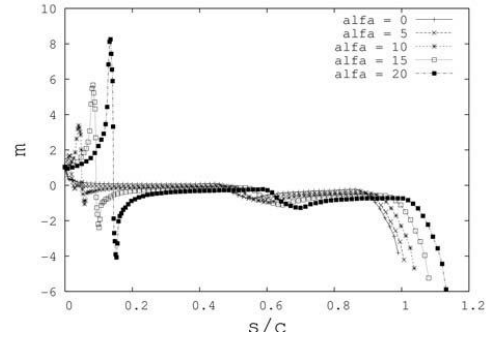

Fig. 4 – Variation of the parameter m with x/c at different angles of attack S 809

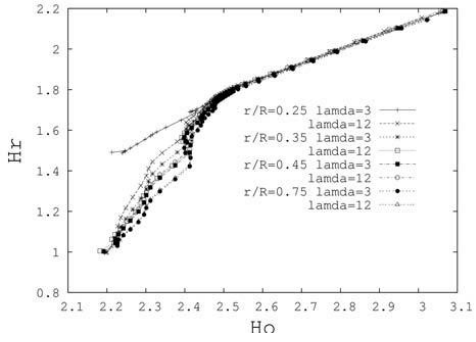

Fig. 5 – Relation between Ho and Hr at r/R=0.25, 0.35, 0.45, 0.75, λ =3,12 α =0 NACA 63-215

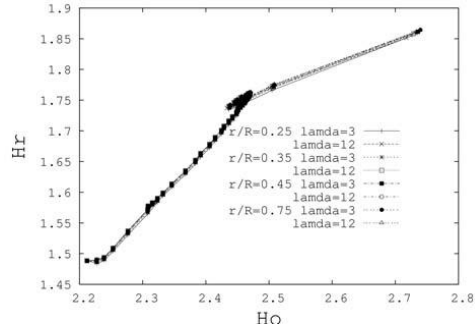

Fig. 6 – Relation between Ho and Hr at r/R=0.25, 0.35, 0.45, 0.75, λ =3,12 α =0 S 809

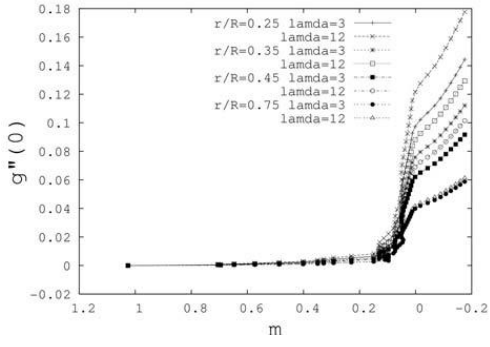

Fig. 7 – Variation of g''(0) with *m* at r/R=0.25, 0.35, 0.45, 0.75, λ =3,12 α =0 NACA 63-215

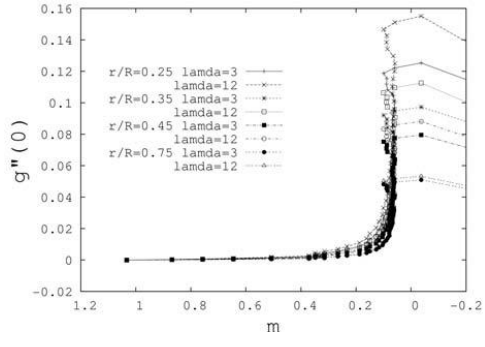

Fig. 8 – Variation of g''(0) with *m* at r/R=0.25, 0.35, 0.45, 0.75, λ =3,12 α =0 S 809

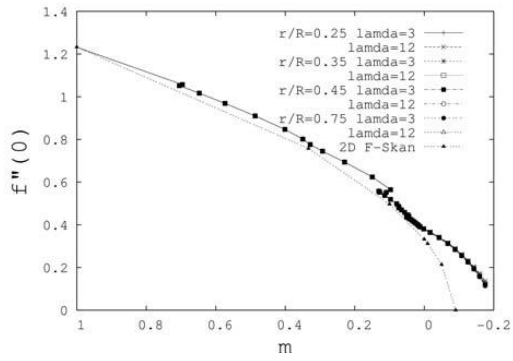

Fig. 9 – Variation of f''(0) with *m* at r/R=0.25, 0.35, 0.45, 0.75, λ =3,12 α =0 NACA 63-215

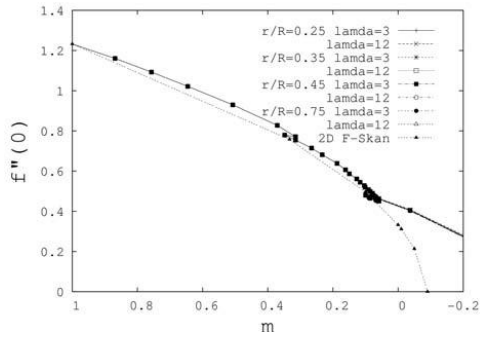

Fig. 10 – Variation of f''(0) with *m* at r/R=0.25, 0.35, 0.45, 0.75, λ =3,12 α =0 S 809

Figure 7 and 8 shows that the skin friction coefficient on the spanwise direction is sensitive to the radial position r/R, the tip speed ratio λ , and the parameter m. As the parameter r/R is increased the rotational effects are less evident, as shown on the figures 7 and 8, small influence on the tip speed ratio λ is observed. It is interesting to note in Figures 9 and 10 that in comparison to the 2D case the velocity profile is more stable in the rotational cases for a given value of m, due to the preventing effect of the cross flow of negative pressure gradients. The spanwise dimensionless pressure-gradient parameter is small but has an important effect before separation occurs. In all cases the separation point is delayed due to the rotational effects. To calculate the stability of the velocity profiles a group of families need to be defined. In the 2D case the skin friction coefficient *f''*(0), the shape factor *H*, or the dimensionless pressure-gradient parameter *m* define a unique family.

To group and map the velocity profiles on the rotating blade, additional parameters are required. The value of *m* similar to the 2D case, with the corresponding skin friction coefficient *f''*(0), since deviations are observed due to the rotation of the blade, see Figures 9 and 10. The skin friction coefficient ratio *g''*(0)/*f''*(0) and the radial position r/R to quantify the rotational effects see Figure 11 and 12. It is interesting to note the influence of the rotational effects, when a favorable pressure gradient is acting on the boundary layer, the skin friction coefficient *f''*(0) is lower than the corresponding 2D case. When the pressure gradient is negative the behavior is similar to Figures 9 and 10. The tangential and cross flow velocity profiles for the tested airfoils can be seen in Figure 13 and 14.

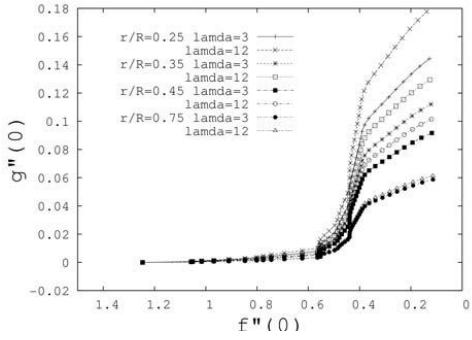

Fig. 11 – Relation between f''(0) and g''(0) at r/R=0.25, 0.35, 0.45, 0.75, λ =3,12 α=0, NACA 63-215

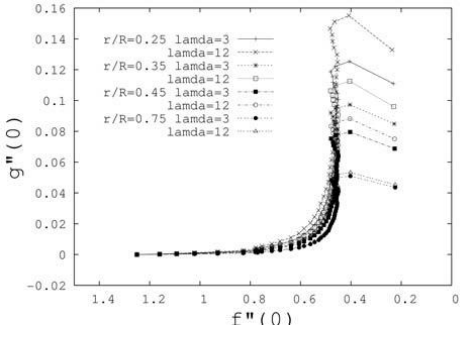

Fig. 12 – Relation between f''(0) and g''(0) at r/R=0.25, 0.35, 0.45, 0.75, λ =3,12, S 809

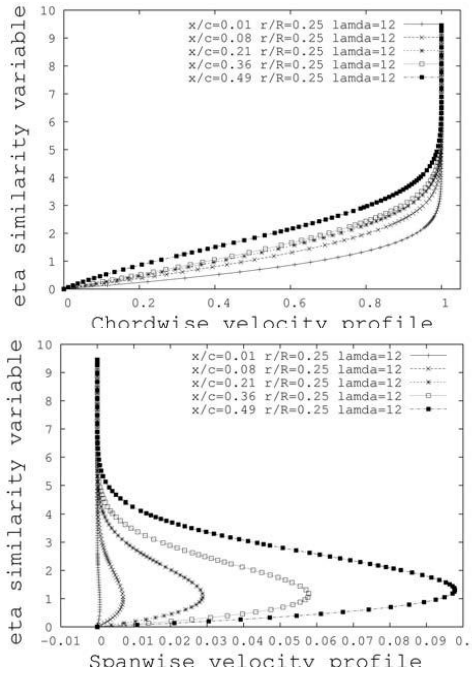

Fig. 13 – Velocity profiles at x/c=0.01-0.49 r/R=0.25 λ =12 α =0 NACA 63-215

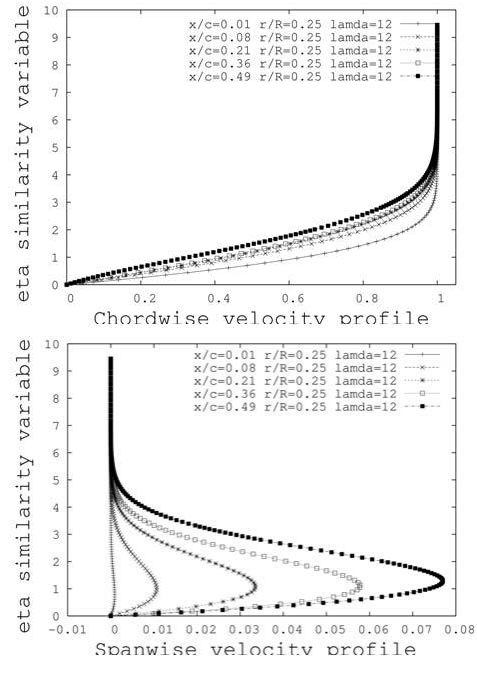

Fig. 14 – Velocity profiles at x/c=0.01-0.49 r/R=0.25 λ =12 α =0, S809

3. CONCLUSIONS

The 3D boundary layer on a rotating wind turbine blade has been solved using a similarity variable approach based on the boundary layer equations in cylindrical coordinates. The three-dimensional inviscid edge-velocity was approached as a decomposition of a relative velocity and a 2D inviscid edge velocity around the cross-sectional airfoil obtained using the XFOIL code. The velocity profiles in the tangential and radial directions have been obtained by solving the boundary layer equations for different pressure gradients, tip-speed-ratios, radial positions and airfoil shapes. Finally, all the velocity profiles have been stored in a database that will be used for predicting transitions on a rotating wind turbine blade in the future.

REFERENCES

[1]. A. G. Hansen, H. Z. Herzig, *Cross flow in laminar incompressible boundary layers* NACA-TN-3651, 1952.
[2]. J.C. Cooke and M. G. Hall, *Boundary layer in three dimensions* Progress in Aero.Sci, vol. **2**, pp. 222-282, 1962.
[3]. H. Snel, *Scaling laws for the boundary layer flow on rotating wind turbine blades*, Proceedings of the fourth IEA symposium on the aerodynamics of wind turbines 1991.
[4]. A. Mager, *Generalization of boundary layer momentum-integral equations to three-dimensional flows including those of a rotating systems*. NACA Report 1967, 1952.
[5]. H. Dumitrescu and V. Cardos, Rotational Effects on the Boundary-Layer Flow in Wind Turbines, *AIAA Journal* **42** (6) 408, 2004.
[6]. Z. Du and M.S. Selig, The effect of rotation on the boundary layer of a wind turbine blade*, Renewable Energy* **20**, pp. 167-181, 2000.

[7]. W. Z. Shen, J. N. Sørensen and R. Mikkelsen, Tip loss correction for Actuator/Navier-Stokes, Computations *Journal of Solar Engineering*, Vol. 127/209, 2005.

[8]. L. E. Fogarty and W. R. Sears, Potential flow solution around a rotating, advancing cylindrical blade, *J. Aero. Sci.* **18** (4), pp. 247, 1951.

[9]. M. Drela, *An analysis and design systems for low Reynolds number airfoils*, Conference on low Reynolds numbers airfoil aerodynamics. University of Notre Dame, June 1989.

[10]. J. Kierzenka and L. F. Shampine *A BVP Solver Based on Residual Control and the MATLAB PSE*, ACM Vol. **27** (3), 1997.

[11]. A.R. Wazzan, T.T. Okamura and A.M.O. Smith, *Spatial and Temporal Stability Charts for The Falkner-Skan Boundary-layer Profiles* Douglas Aircraft Co. Report DAC-67086, 1968.